RESEARCH ARTICLE

Arc-Tangent Exponential Distribution With Applications to Weather and Chemical Data Under Classical and Bayesian Approach

LAXMI PRASAD SAPKOTA[1], ARWA M. ALSAHANGITI[2], VIJAY KUMAR[3], AHMED M. GEMEAY[4], M. E. BAKR[2], OLUWAFEMI SAMSON BALOGUN[5], AND ABDISALAM HASSAN MUSE[6]

[1]Department of Statistics, Tribhuvan University, Tribhuvan Multiple Campus, Tansen, Palpa, Lumbini 44600, Nepal
[2]Department of Statistics and Operations Research, College of Science, King Saud University, P.O. Box 2455, Riyadh 11451, Saudi Arabia
[3]Department of Mathematics and Statistics, DDU Gorakhpur University, Gorakhpur, Uttar Pradesh 273001, India
[4]Department of Mathematics, Faculty of Science, Tanta University, Tanta 31527, Egypt
[5]Department of Computing, University of Eastern Finland, 70211 Kuopio, Finland
[6]Faculty of Science and Humanities, School of Postgraduate Studies and Research (SPGSR), Amoud University, Borama 25263, Somalia

Corresponding author: Abdisalam Hassan Muse (abdisalam.hassan@amoud.edu.so)

ABSTRACT This paper introduces the Arctan exponential distribution, a novel two-parameter trigonometric distribution. Various statistical properties of the distribution are examined, including hazard rate functions, cumulative hazard rate functions, mean deviation, reliability function, moments, conditional moments, incomplete moments, quantile function, entropy, Lorenz and Bonferroni curves, order statistics, and symmetry measures such as skewness and kurtosis. The parameters of the proposed distribution are estimated using the maximum likelihood estimation method, and a simulation study is conducted to assess its performance. Two real datasets are utilized to demonstrate the significance of the proposed distribution, showing that it performs comparably or better than well-known distributions. Furthermore, the suggested Arctan exponential distribution is employed within the Bayesian framework. The model's parameters are estimated and predicted using posterior samples generated through the application of the Markov Chain Monte Carlo (MCMC) technique. The application of the suggested model involves employing the Stan software in conjunction with the Hamiltonian Monte Carlo (HMC) algorithm and its adaptive variant known as the No-U-turn sampler (NUTS). A real dataset is utilized to showcase the methodology, and both numerical and graphical Bayesian analyses are performed, employing weakly informative priors. A posterior predictive check is also conducted to evaluate the model's predictability. The tools and methods employed in this study adhere to the Bayesian approach and are implemented using the R statistical programming language.

INDEX TERMS Arctan distribution, posterior distribution, gamma prior, credible interval, Lorenz curve.

I. INTRODUCTION

Statistical distributions play a pivotal role in the field of probability theory and statistics, providing a mathematical framework to describe the behavior of random variables and the likelihood of various outcomes in a given dataset or phenomenon. These distributions are fundamental building blocks for various statistical analyses and inference

The associate editor coordinating the review of this manuscript and approving it for publication was Shuangqing Wei.

techniques. By characterizing the patterns and variability of data, statistical distributions enable researchers and analysts to make informed decisions, draw meaningful conclusions, and quantify uncertainties in their findings. Each distribution possesses unique properties and parameters that capture specific data characteristics, such as central tendency, spread, and shape. The selection of an appropriate distribution depends on the nature of the data and the research question at hand. Gaussian (normal), exponential, binomial, Poisson, and uniform distributions, among others, find extensive

applications in fields such as economics, biology, engineering, and social sciences. Through their ability to model real-world phenomena and provide a structured framework for data analysis, statistical distributions are indispensable tools for researchers and practitioners seeking to derive insights and make evidence-based inferences from empirical observations.

Statistical models have emerged as indispensable tools in the fields of weather and chemistry due to their capacity to discern patterns, relationships, and trends within complex datasets. In meteorology, these models aid in forecasting and understanding atmospheric phenomena by integrating diverse variables such as temperature, humidity, and air pressure to predict weather patterns. They enable researchers to unravel the dynamics of climate change, extreme events, and long-term trends, providing valuable insights for policy formulation and disaster preparedness. Similarly, in chemistry, statistical models contribute to the analysis of intricate molecular interactions, aiding in drug discovery, environmental assessments, and material design. By capturing intricate correlations among various chemical properties, these models facilitate the prediction of chemical behaviors and reactions. Moreover, they optimize experiments, reduce costs, and offer a deeper understanding of the underlying mechanisms. In both weather and chemistry, statistical models bridge the gap between observations and theoretical understanding, enhancing decision-making processes and advancing scientific knowledge.

Probability distributions are frequently employed to examine the lifespan of events, devices, or system components. Lifetime distributions find wide application across various fields, including medicine, biology, econometrics, engineering, and insurance. Several well-known classical continuous probability distributions have been identified in statistical literature for analyzing lifetime datasets. These include the exponential, Cauchy, gamma, Weibull, etc. distributions. Over the past few years, researchers have predominantly focused on the exponential distribution's ability to model lifetime data. Its closed-form solutions have proven highly effective in numerous reliability analyses. However, it is important to note that while the exponential distribution assumes a constant failure rate, real-world failure rates often deviate from this assumption. Consequently, using an exponential distribution may often be inappropriate and unrealistic. Recently, researchers have endeavored to develop novel probability distributions that extend existing ones, providing greater flexibility in data modeling. These distributions are created by introducing new parameters into established distributions, thus expanding the family of distributions available. In the past few years, modifications to the original exponential distribution introduced by Smith and Bain [37] have been proposed, resulting in the emergence of the exponential power distribution. These models have been instrumental in establishing novel classes of distributions. For instance, Gupta and Kundu [16] devised a generalized exponential distribution that surpasses the standard exponential

model by incorporating a hazard function with varying failure rates.

Gupta and Kundu [17] also introduced the weighted exponential distribution, while Y AL-Jammal [1] proposed the exponentiated exponential distribution to model failure data. In [7], the exponential-Weibull distribution was introduced as a suitable model for skewed lifetime data. To extend the exponential distribution, Chaudhary et al. [5] proposed the truncated version of the Cauchy power exponential distribution, and Joshi et al. [24] proposed the logistic-exponential power distribution, which uses exponential power as a parent distribution. If the random variable i.e. $X > 0$ follows an exponential distribution with parameter λ, then its cumulative distribution function (CDF) and probability density function (PDF) are

$$G(x; \lambda) = 1 - \exp(-\lambda x) \; ; \lambda > 0. \tag{1}$$
$$g(x; \lambda) = \lambda \exp(-\lambda x) \; ; \lambda > 0. \tag{2}$$

Nadarajah and Haghighi [30] proposed the extended exponential distribution as an expansion of the exponential distribution. Due to its broad application, simplicity, and mathematical tractability, we chose the exponential distribution as the base distribution. We present a trigonometric model in this study. Recently, trigonometric models have attracted significant attention from researchers. For instance, Souza et al. [38] introduced the Sine inverse Weibull distribution, and Jamal and Chesneau [23] proposed the Sine Kumaraswamy-G family and analyzed the Sine Kumaraswamy exponential distribution. Furthermore, Shrahili et al. [36] introduced the Sine inverted exponential distribution, and Tomy and Chesneau [41] defined the Sine modified Lindley distribution using the Sine-G family of distribution. Additionally, Chaudhary et al. [6] presented the arctan generalized exponential distribution with a flexible hazard rate, and Isa et al. [22] defined the Sine exponential distribution and investigated its properties. Its CDF and PDF respectively are as follows

$$G(x; \beta) = \sin\left[\frac{\pi}{2}\left(1 - e^{-\beta x}\right)\right]; x > 0, \beta > 0, \tag{3}$$

and

$$g(x; \beta) = \frac{\pi}{2}\beta e^{-\beta x}\cos\left[\frac{\pi}{2}\left(1 - e^{-\beta x}\right)\right]; x > 0, \beta > 0. \tag{4}$$

The primary goal of this paper is to introduce a versatile trigonometric model that can be fitted to real-world data by inserting one more parameter into the exponential distribution. Trigonometric models are relatively recent in the area of statistics and reliability analysis, and we are interested in exploring their properties. To accomplish this, we have opted to utilize the arc-tan-G family of distribution presented by Gómez-Déniz and Calderín-Ojeda [15] to introduce our new model. They initially introduced this distribution family to model Norwegian fire insurance data and proposed the Pareto arctan distribution as a new distribution based on an underlying Pareto distribution. It was observed that this

distribution provided a better fit when compared to other established distributions. The Arctan distribution family's CDF and PDF have also been provided with support [a, b].

$$F(x) = 1 - \frac{\arctan[\alpha\{1 - G(x;\tau)\}]}{\arctan(\alpha)}; \alpha > 0, x \geqslant 0; \alpha \in [a,b].$$

(5)

$$f(x) = \frac{1}{\arctan(\alpha)} \frac{\alpha g(x;\tau)}{1 + [\alpha\{1 - G(x;\tau)\}]^2}; \alpha > 0, x \geqslant 0.$$

(6)

Here $g(x;\tau)$ and $G(x;\tau)$ are the PDF and CDF of an arbitrary parent model respectively. The parameter space of the parent model is denoted by τ. In this paper, the authors have employed both the classical and Bayesian approaches for parameter estimation, posterior analysis, and posterior predictive check. A comprehensive Bayesian approach was implemented using Markov Chain Monte Carlo (MCMC) methods, specifically the Hamiltonian Monte Carlo (HMC) algorithm and its adaptive variant, the No-U-turn sampler (NUTS), to investigate this model. For more details, see [8], [25], and [31]. The proposed study is divided into several sections. Section II introduces the arctan exponential distribution and several reliability-related functions. Section III discusses the statistical properties of the proposed model. To compute the model's parameters, the maximum likelihood estimation (MLE) method is used in Section IV. In Section V, we perform a simulation study to investigate the characteristics of the MLEs. In Section VI, we evaluate the applicability of the proposed distribution using two real-world data sets. Here, we assess the goodness of fit and model adequacy through various tests to validate the arctan exponential model. Bayesian analysis of the suggested model is presented in Section VII and finally, we provide some general concluding remarks in Section VIII.

II. THE ARCTAN EXPONENTIAL (ATE) DISTRIBUTION

By inserting Equation (1) into Equation (5), the CDF of the ATE distribution can be obtained with the parameters α and λ. This can then be presented as:

$$F(x;\alpha,\lambda) = 1 - \frac{\arctan[\alpha\{\exp(-\lambda x)\}]}{\arctan(\alpha)}; \alpha, \lambda > 0, x \geqslant 0.$$

(7)

And the corresponding PDF of Equation (8) is

$$f(x;\alpha,\lambda) = \frac{\alpha\lambda}{\arctan(\alpha)} \left\{ \frac{\exp(-\lambda x)}{1 + [\alpha\exp(-\lambda x)]^2} \right\}; x \geqslant 0.$$

(8)

A. RELIABILITY FUNCTION

Let $X \sim ATE\left(\alpha,\lambda\right)$ then the function for the reliability of ATE distribution is

$$R(x) = \frac{\arctan[\alpha\{\exp(-\lambda x)\}]}{\arctan(\alpha)}; x \geqslant 0.$$

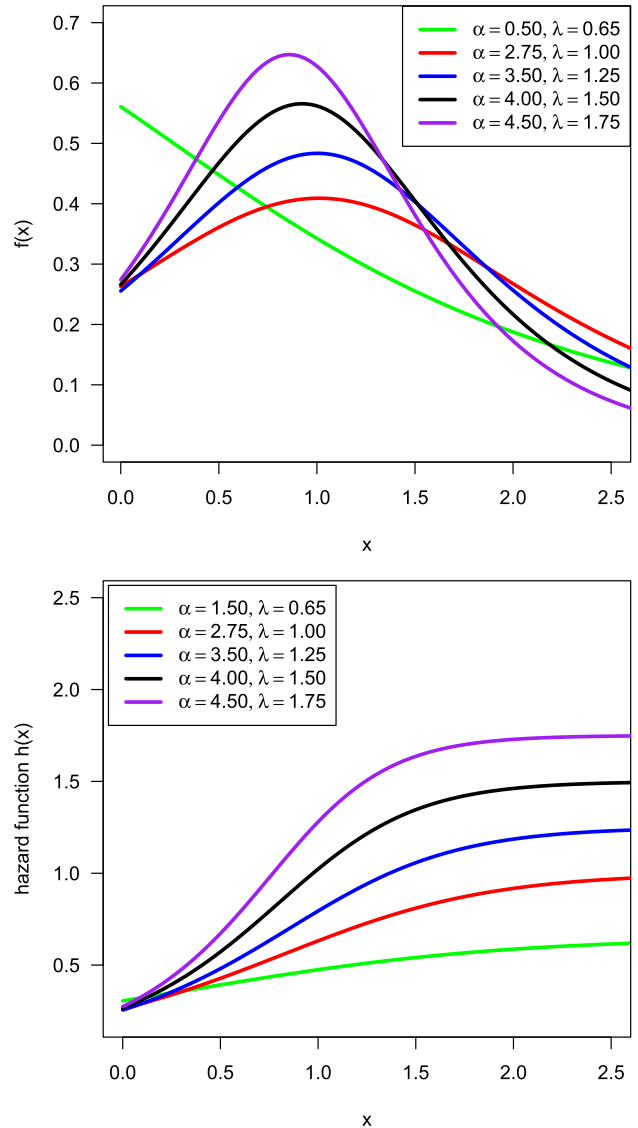(9)

FIGURE 1. Possible shapes of PDF (on the left) and HRF (on the right) for various α and λ values.

B. HAZARD RATE FUNCTION (HRF)

Let $X \sim ATE\left(\alpha,\lambda\right)$ then HRF of ATE distribution is,

$$h(x) = \frac{\alpha\lambda e^{-\lambda x}}{\arctan\left[\alpha\{\exp(-\lambda x)\}\right]\left\{1 + [\alpha\exp(-\lambda x)]^2\right\}}; x \geqslant 0.$$

(10)

C. HAZARD DISTRIBUTION FUNCTION

For the proposed model, it can be expressed as

$$H(x) = -\log\left[\frac{\arctan[\alpha\{\exp(-\lambda x)\}]}{\arctan(\alpha)}\right].$$

(11)

Graphs of the ATE distribution's PDF and HRF for different α and λ parameter values are shown in Figure 1.

III. STATISTICAL PROPERTIES OF ATE DISTRIBUTION
A. LINEAR FORM OF ATE DISTRIBUTION
To enhance the understanding of the ATE distribution, we utilize power series expansions to extend both its CDF and PDF.

$$(1-y)^n = \sum_{j=0}^{n} (-1)^j \binom{n}{j} y^j; |y| < 1, n > 0. \quad (12)$$

$$(1+y)^{-n} = \sum_{j=0}^{n} (-1)^j \binom{n+j-1}{j} y^j. \quad (13)$$

Expansion of the CDF of ATE distribution defined in (7) is

$$[F(x)]^k = \left[1 - \frac{\arctan[\alpha\{\exp(-\lambda x)\}]}{\arctan(\alpha)}\right]^k. \quad (14)$$

Applying series (12) we can express as

$$[F(x)]^k = \sum_{j=0}^{\infty} d_j \left\{\arctan(\alpha e^{-\lambda x})\right\}^j. \quad (15)$$

where $d_j = (-1)^j \binom{k}{j} \{\arctan(\alpha)\}^{-j}$ The PDF defined in Equation (8) takes the form

$$f(x) = \frac{\alpha\lambda}{\arctan(\alpha)} \left\{1 + [\alpha \exp(-\lambda x)]^2\right\}^{-1} \exp(-\lambda x). \quad (16)$$

Using Equation (13) we can obtain

$$f(x) = \sum_{i=0}^{\infty} \varepsilon_i e^{-\lambda(2i+1)x}. \quad (17)$$

where $\varepsilon_i = \frac{(-1)^i \alpha^{1+2i}\lambda}{\arctan\alpha}$. Further, the PDF defined in Equation (17) can also be presented as the linear combination of exponential densities as

$$f(x) = \frac{1}{\arctan\alpha} \sum_{i=0}^{\infty} (-1)^i \alpha^{2i+1} \lambda\, e^{-\lambda(2i+1)x}$$

$$= \frac{1}{\arctan\alpha} \sum_{i=0}^{\infty} (-1)^i \frac{\alpha^{2i+1}}{(2i+1)} \lambda (2i+1)\, e^{-\lambda(2i+1)x}$$

$$= \frac{1}{\arctan\alpha} \sum_{i=0}^{\infty} (-1)^i \frac{\alpha^{2i+1}}{(2i+1)} f^*(x). \quad (18)$$

Here $f^*(x)$ denote the PDF of exponential distribution with rate parameter $\lambda(2i+1)$.

B. MOMENTS OF ATE DISTRIBUTION
The rth moment about the origin of ATE distribution using PDF defined in Equation (17) can be defined as

$$\mu'_r = \int_0^{\infty} x^r f(x)\,dx$$

$$= \int_0^{\infty} x^r \sum_{i=0}^{\infty} \varepsilon_i e^{-\lambda(1+2i)x}\,dx$$

$$= \sum_{i=0}^{\infty} \varepsilon_i \frac{\Gamma(r+1)}{[\lambda(1+2i)]^{r+1}}. \quad (19)$$

where $\int_0^{\infty} x^n e^{-ax}\,dx = \frac{\Gamma(n+1)}{a^{n+1}}$ is a standard gamma integral. Substituting the values of $r = 1, 2, 3, 4$ in Equation (19) we get the first four moments. Now one can compute the mean of X as

$$E(X) = \mu'_1 = \sum_{i=0}^{\infty} \varepsilon_i \frac{1}{[\lambda(1+2i)]^2}.$$

C. CONDITIONAL MOMENTS
The qth conditional moment of ATE distribution can be determined as

$$\gamma_q = \int_a^{\infty} x^q f(x)\,dx$$

$$= \int_a^{\infty} x^q \sum_{i=0}^{\infty} \varepsilon_i e^{-\lambda(1+2i)x}\,dx$$

$$= \sum_{i=0}^{\infty} \varepsilon_i \frac{\Gamma(q+1, \lambda(1+2i)a)}{[\lambda(1+2i)]^{q+1}}, \quad (20)$$

where $\int_a^{\infty} x^n e^{-bx}\,dx = \frac{\Gamma(n+1, ab)}{b^{n+1}}$ is an upper gamma integral function and $\varepsilon_i = \frac{(-1)^i \alpha^{1+2i}\lambda}{\arctan\alpha}$.

D. INCOMPLETE MOMENT
The utilization of incomplete moments is significant in assessing reliability. The rth incomplete moment of the ATE distribution can be formulated as follows:

$$M_r^{inc} = \int_0^t x^r f(x)\,dx$$

$$= \sum_{i=0}^{\infty} \varepsilon_i \frac{\gamma(r+1, \lambda(2i+1)t)}{\{\lambda(2i+1)\}^{r+1}}, \quad (21)$$

where $\gamma(a, b) = \int_0^b e^{-x} x^{a-1}\,dx$ is the function of lower incomplete gamma.

E. MOMENT GENERATING FUNCTION (MGF) OF ATE DISTRIBUTION
The mgf of Y using Equation (19) is

$$M_Y(t) = E(e^{tY}) = \sum_{k=0}^{\infty} \frac{t^k}{k!} \mu'_k$$

$$= \sum_{k=0}^{\infty} \sum_{i=0}^{\infty} \varepsilon_i \frac{t^k}{k!} \Gamma(k+1) [\lambda(1+2i)]^{-(k+1)}. \quad (22)$$

F. INEQUALITY MEASUREMENT FUNCTIONS
1) LORENZ CURVE (LC)
It is also an important statistical tool to measure inequality, and it can be obtained for ATE distribution as

$$L(p) = \frac{M_1^{inc}(p)}{\mu'_1} = \sum_{i=0}^{\infty} \gamma(2, \lambda(2i+1)p), \quad (23)$$

where M_1^{inc} is the first incomplete moment and p is the quantile function.

2) BONFERRONI CURVE (BC)

This function can be obtained by using LC and defined as $B(p) = \frac{L(p)}{p}$.

G. ENTROPY

Entropy is a statistical tool used to quantify the degree of randomness or variation. Two commonly used entropies, *Renyi*, and *q*, have been developed for ATE distribution.

1) RENYI ENTROPY

This type of entropy can be defined as

$$I_h(x) = \frac{1}{1-h} \log \int_0^\infty [f(x)]^h \, dx \; ; h > 0 \text{ and } h \neq 1. \quad (24)$$

The expression for $[f(x)]^h$ is derived as

$$[f(x)]^h = \sum_{i=0}^\infty v_i e^{-\lambda(h+2i)x}.$$

where $v_i = \dfrac{(-1)^i \binom{h+i-1}{i} \alpha^h \lambda^h}{(\arctan \alpha)^h}$. Now Renyi entropy for ATE distribution is

$$I_h(x) = \frac{1}{1-h} \log \left[\sum_{i=0}^\infty v_i \frac{1}{\lambda(h+2i)} \right]; \; h > 0 \text{ and } h \neq 1. \quad (25)$$

2) Q-ENTROPY

Similarly, q-entropy is defined as

$$Z_q(x) = \log \left[1 - \int_0^\infty [f(x)]^q \, dx \right] (1-q)^{-1}; q > 0 \text{ and } q \neq 1. \quad (26)$$

$$Z_q(x) = \log \left[1 - \sum_{i=0}^\infty v_i \frac{1}{\lambda(q+2i)} \right] (1-q)^{-1}. \quad (27)$$

H. MEAN DEVIATION (MD)

The expression for MD about the mean is

$$MD(\mu) = \int_0^\infty |x - \mu| f(x) dx$$

$$= 2\mu F(\mu) - 2\mu + \int_\mu^\infty x f(x) dx, \quad (28)$$

where μ is the $E(X)$. Using the PDF defined in Equation (17) and the upper gamma function defined in Equation (20) we get

$$MD(\mu) = 2\mu F(\mu) - 2\mu + \sum_{i=0}^\infty \varepsilon_i \frac{\Gamma\{2, \lambda(1+2i)\mu\}}{\lambda^2 (1+2i)^2}. \quad (29)$$

I. ORDER STATISTICS (OS) FOR ATE DISTRIBUTION

Let $X_{i:n}$ denotes the ith OS and $f_{i:n}$ denotes PDF of ith OS for $X_{(1)}, \ldots, X_{(n)}$ from CDF $F_{i:n}(x)$ and using CDF and PDF defined in Equations (15) and (17) and PDF of OS for ATE is

$$f_{i:n}(x) = \frac{n!}{(i-1)!(n-i)!} [1 - F(x)]^{n-i} [F(x)]^{i-1} f(x)$$

$$= \frac{n!}{(i-1)!(n-i)!} f(x) \sum_{c=1}^{n-i} \binom{n-i}{c} [F(x)]^{c+i-1}$$

$$= \frac{n!}{(i-1)!(n-i)!} \sum_{k=0}^\infty \sum_{j=0}^\infty \sum_{c=1}^{n-i} \binom{n-i}{c} d_j \varepsilon_k \, e^{-\lambda(1+2k)x}$$

$$\left\{ \arctan(\alpha e^{-\lambda x}) \right\}^j, \quad (30)$$

where $d_j = (-1)^j \binom{c+i-1}{j} \{\arctan(\alpha)\}^{-j}$ and $\varepsilon_k = \frac{(-1)^k \alpha^{1+2k} \lambda}{\arctan \alpha}$.

J. QUANTILE FUNCTION (QF) FOR ATE DISTRIBUTION

QF of the ATE distribution with u following a uniform distribution $[0, 1]$ is composed as

$$Q(u; \alpha, \lambda) = -\frac{1}{\lambda} \log \left[\frac{1}{\alpha} tan\{arctan(\alpha)(1-u)\} \right]; 0 < u < 1. \quad (31)$$

By substituting the value of $u = 1/4, 1/2$ and $3/4$ in Equation (31) we can obtain the value of the lower quartile, median and upper quartile respectively.

K. RANDOM DEVIATION GENERATION

Using the quantile function, we can generate random numbers as

$$x = -\frac{1}{\lambda} \log \left[\frac{1}{\alpha} tan\{(1-v)arctan(\alpha)\} \right]; 0 < v < 1. \quad (32)$$

L. SKEWNESS AND KURTOSIS

Skewness and kurtosis are effective statistical techniques for conducting descriptive analyses. To compute Bowley's skewness utilizing quantiles, we can use the following formula:

$$B_{SK} = \frac{Q(0.25; \alpha, \lambda) - 2Q(0.5; \alpha, \lambda) + Q(0.75; \alpha, \lambda)}{Q(0.75; \alpha, \lambda) - Q(0.5; \alpha, \lambda)}. \quad (33)$$

and The Moors kurtosis introduced by Moors [28] is (34), as shown at the bottom of the next page.

From Figure 2, it can be observed that the ATE distribution's skewness and kurtosis decrease with increasing values of the parameter α. Additionally, it appears that λ has a minimal effect on the shape of the distribution.
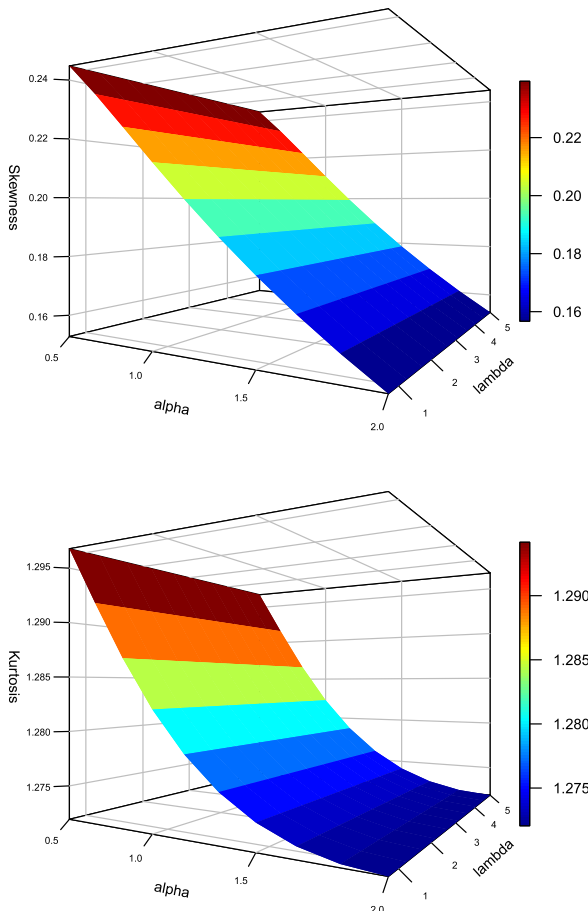
FIGURE 2. Graphs of skewness and kurtosis for different combination of α and λ.

IV. CLASSICAL METHODS FOR PARAMETER ESTIMATION
A. MLE METHOD
In this part, we have demonstrated the MLE method to estimate the parameters of the ATE distribution. The log-likelihood function $l\left(\alpha, \lambda / \underline{x}\right)$ for the random sample $\underline{x} = (x_1, \ldots, x_n)$ of size 'n' from $ATE\left(\alpha, \lambda\right)$ can be presented as,

$$l\left(\alpha, \lambda | \underline{x}\right) = n\left(\log \alpha + \log \lambda\right) - n \log\{arctan(\alpha)\} - \lambda \sum_{i=1}^{n} x_i$$

$$- \sum_{i=1}^{n} \ln\left\{1 + [\alpha \exp(-\lambda x_i)]^2\right\}. \quad (35)$$

By differentiating Equation (35) with respect to α, and λ we get

$$\frac{\partial l}{\partial \alpha} = \frac{n}{\alpha} - \frac{n}{\arctan(\alpha)[1+\alpha^2]} - 2\alpha \sum_{i=1}^{n} \frac{[\exp(-\lambda x_i)]^2}{1 + [\alpha \exp(-\lambda x_i)]^2}. \quad (36)$$

$$\frac{\partial l}{\partial \lambda} = \frac{n}{\lambda} - \sum_{i=1}^{n} x_i - 2\alpha^2 \sum_{i=1}^{n} \frac{x_i[\exp(-\lambda x_i)]^2}{1 + [\alpha \exp(-\lambda x_i)]^2}. \quad (37)$$

The MLEs for ATE will be acquired by solving Equations (36) and (37) and setting the unknown parameters (α, λ) to zero. As resolving them manually is challenging, one can utilize the appropriate software to solve these equations.

B. CONFIDENCE INTERVAL (CI) FOR PARAMETERS
Let $\underline{\mho} = (\alpha, \lambda)$ and $\widehat{\underline{\mho}} = (\hat{\alpha}, \hat{\lambda})$, denote the vectors for parameters and MLEs then the information matrix defined by Fisher is obtained as

$$I\left(\underline{\mho}\right) = - \begin{pmatrix} E\left(\frac{\partial^2 l}{\partial \alpha^2}\right) & E\left(\frac{\partial^2 l}{\partial \alpha \partial \lambda}\right) \\ E\left(\frac{\partial^2 l}{\partial \lambda \partial \alpha}\right) & E\left(\frac{\partial^2 l}{\partial \lambda^2}\right) \end{pmatrix} \quad (38)$$

Now the observed matrix $O\left(\widehat{\underline{\mho}}\right)$ can be used as an estimate of $I\left(\underline{\mho}\right)$

$$O\left(\widehat{\underline{\mho}}\right) = - \begin{pmatrix} \frac{\partial^2 l}{\partial \alpha^2} & \frac{\partial^2 l}{\partial \alpha \partial \lambda} \\ \frac{\partial^2 l}{\partial \lambda \partial \alpha} & \frac{\partial^2 l}{\partial \lambda^2} \end{pmatrix}_{|\left(\hat{\alpha}, \hat{\lambda}\right)} = -Z\left(\underline{\mho}\right)_{|_{\left(\underline{\mho}=\widehat{\underline{\mho}}\right)}} \quad (39)$$

where Z is a Hessian matrix. Hence inverse of the observed matrix is used to generate the SE as

$$\left[-Z\left(\underline{\mho}\right)_{|_{\left(\underline{\mho}=\widehat{\underline{\mho}}\right)}}\right]^{-1} = \begin{pmatrix} var(\hat{\alpha}) & cov(\hat{\alpha}, \hat{\lambda}) \\ cov(\hat{\lambda}, \hat{\alpha}) & var(\hat{\lambda}) \end{pmatrix}. \quad (40)$$

Hence the CI at $100(1 - v)\%$ confidence levels for parameters (α, λ) can be presented as follows: $\hat{\alpha} \pm \eta_{v/2} SE\left(\hat{\alpha}\right)$, and $\hat{\lambda} \pm \eta_{v/2} SE\left(\hat{\lambda}\right)$ where $\eta_{v/2}$ is the area under the normal curve.

V. NUMERICAL SIMULATION FOR MLES
The behavior of the MLEs of the $ATE(\alpha, \lambda)$ distribution can be studied using Monte Carlo simulation for $N = 1000$ replications. In this study, we select sample sizes $n = 20, 40, 60, 80, 100, 150$ and two sets of parameter combinations. To carry out this study, we have performed the following algorithm
1) Assign the initial values to the parameter.
2) Decide the size of the sample n.
3) Using the quantile function, generate the random numbers of size n.
4) Determine the MLEs of each of N independent samples.
5) Determine the mean of the N estimates and calculate the biases and mean square error (MSE) for each parameter as

$Bias = \frac{1}{N} \sum_{k=1}^{N} (\alpha_i - \alpha))$ and $MSE = \frac{1}{N} \sum_{k=1}^{N} (\alpha_i - \alpha)^2$ for α, where α is the initial value and similarly for λ. Results of the

$$M_{KU} = \frac{Q\left(0.375; \alpha, \lambda\right) - Q\left(0.625; \alpha, \lambda\right) + Q\left(0.875; \alpha, \lambda\right) - Q\left(0.125; \alpha, \lambda\right)}{Q\left(0.75; \alpha, \lambda\right) - Q\left(0.25; \alpha, \lambda\right)} \quad (34)$$

TABLE 1. Simulation study for $\alpha = 0.5$ and $\lambda = 0.25$.

n	MLE		Bias		MSE	
	$\hat{\alpha}$	$\hat{\lambda}$	$\hat{\alpha}$	$\hat{\lambda}$	$\hat{\alpha}$	$\hat{\lambda}$
20	1.0491	0.3045	0.5491	0.0545	2.016	0.0131
40	0.7527	0.2794	0.2527	0.0294	0.6514	0.0047
60	0.6399	0.2697	0.1399	0.0197	0.3942	0.0027
80	0.596	0.2649	0.096	0.0149	0.3022	0.0017
100	0.5684	0.2619	0.0684	0.0119	0.2719	0.0012
150	0.5213	0.2577	0.0213	0.0077	0.1766	0.0008

TABLE 2. Simulation study for $\alpha = 0.75$ and $\lambda = 0.5$.

n	MLE		Bias		MSE	
	$\hat{\alpha}$	$\hat{\lambda}$	$\hat{\alpha}$	$\hat{\lambda}$	$\hat{\alpha}$	$\hat{\lambda}$
20	1.2757	0.5988	0.5257	0.0988	2.439	0.0488
40	0.9592	0.5509	0.2092	0.0509	0.7664	0.0177
60	0.855	0.5327	0.105	0.0327	0.4573	0.0105
80	0.8115	0.5235	0.0615	0.0235	0.351	0.0067
100	0.7895	0.5179	0.0395	0.0179	0.3123	0.005
150	0.7538	0.5108	0.0038	0.0108	0.1976	0.0032

TABLE 3. Simulation study for *alpha* = 1.25 and *lambda* = 0.75.

n	MLE		Bias		MSE	
	$\hat{\alpha}$	$\hat{\lambda}$	$\hat{\alpha}$	$\hat{\lambda}$	$\hat{\alpha}$	$\hat{\lambda}$
20	1.9459	0.8727	0.6959	0.1227	4.3805	0.0926
40	1.4378	0.793	0.1878	0.043	0.9301	0.0289
60	1.4421	0.7869	0.1921	0.0369	0.7002	0.0209
80	1.3451	0.7743	0.0951	0.0243	0.4696	0.0153
100	1.3291	0.7694	0.0791	0.0194	0.3231	0.0107
150	1.2968	0.7613	0.0468	0.0113	0.2087	0.0075

TABLE 4. Simulation study for $\alpha = 1.5$ and $\lambda = 1.25$.

n	MLE		Bias		MSE	
	$\hat{\alpha}$	$\hat{\lambda}$	$\hat{\alpha}$	$\hat{\lambda}$	$\hat{\alpha}$	$\hat{\lambda}$
20	2.2749	1.4317	0.7749	0.1817	5.0486	0.236
40	1.8238	1.3346	0.3238	0.0846	1.6174	0.0982
60	1.6869	1.3013	0.1869	0.0513	0.8061	0.0579
80	1.6141	1.2805	0.1141	0.0305	0.5253	0.0396
100	1.599	1.2811	0.099	0.0311	0.386	0.0319
150	1.5468	1.2689	0.0468	0.0189	0.2588	0.0198

TABLE 5. CI for MLEs along with SE.

Parameter	CI	MLE	SE
α	(0.5019, 11.5400)	6.0246	2.814
λ	(0.8193, 1.7659)	1.2926	0.2415

C. TEST OF THE ADEQUACY OF ATE DISTRIBUTION

To illustrate the performance of the ATE distribution, we selected several renowned distributions for comparative analysis. These distributions include the Gompertz distribution (GZ) introduced by Murthy et al. [29], the Exponential power (EP) distribution proposed by Smith and Bain [37], the Marshall-Olkin Extended Exponential (MOEE) distribution presented by Marshall and Olkin [26], and the NHE distribution (Exponential extension) by Nadarajah and Haghighi [30].

To assess the model adequacy, we computed various information criteria: the Akaike information criterion (AIC), corrected AIC (CAIC), negative log-likelihood (-LL), Bayesian information criterion (BIC), and Hannan-Quinn information criterion (HQIC). These criteria were calculated using the following expressions:

$$AIC = -2l(\hat{\theta}) + 2b.$$
$$BIC = -2l(\hat{\theta}) + b\log(n).$$
$$CAIC = AIC + \frac{2b(w+1)}{n-b-1}.$$
$$HQIC = -2l(\hat{\theta}) + 2b\log\left[\log(n)\right].$$

where the symbols n and b, represent the sample size and the number of parameters respectively. To evaluate the adequacy of fit for the ATE distribution, we computed three statistical metrics: Kolmogorov-Smirnov (KS), Anderson-Darling (W), and Cramer-Von Mises (A^2). These tests are commonly used to compare models and assess the level of agreement between an observed dataset's empirical distribution and a particular cumulative distribution function (CDF).

$$KS = \max_{1 \leqslant i \leqslant n} \left(d_i - \frac{i-1}{n}, \frac{i}{n} - d_i \right),$$
$$W = -n - \frac{1}{n} \sum_{i=1}^{n} (2i-1)\left[\log d_i + \log(1 - d_{n+1-i})\right],$$
$$A^2 = \frac{1}{12n} + \sum_{i=1}^{n} \left[\frac{(2i-1)}{2n} - d_i\right]^2,$$

where $d_{(i)} = CDF(x_{(i)})$ the x_i's are ordered variables. Table 6 displays the AIC, BIC, CAIC, HQIC, and -LL

simulation are presented in Tables 1 and 2 and we observed that biases and MSEs are decreased even for small increments in the sample size.

VI. APPLICATIONS TO REAL DATASET

For the application, we demonstrate the usefulness of ATE distribution by showcasing two real authentic datasets: meteorology and chemistry.

A. DATASET-I

We used an actual data set that was first employed by Hinkley [19]. The dataset provides thirty consecutive March rainfall (inches) values for Minneapolis/St. Paul. "0.77, 1.74, 0.81, 1.20, 1.95, 1.20, 0.47, 1.43, 3.37, 2.20, 3.00, 3.09, 1.51, 2.10, 0.52, 1.62, 1.31, 0.32, 0.59, 0.81, 2.81, 1.87, 1.18, 1.35, 4.75, 2.48, 0.96, 1.89, 0.90, 2.05"

B. ESTIMATION OF THE PARAMETERS

The MLEs were calculated by optimizing the likelihood function (35) through the function `maxLik()` in the R software package [34], as described by Hui [21]. The MLEs, along with their SE and 95%CI for α and λ, are presented in Table 5. Also, we have calculated the matrix for variance as

$$M = \begin{bmatrix} 7.91837 & 0.56158 \\ 0.56158 & 0.05835 \end{bmatrix}$$

TABLE 6. Some model selection statistics.

Distribution	AIC	BIC	CAIC	HQIC	-LL
ATE	82.4562	85.2585	82.9006	83.3527	39.2281
MOEE	82.7540	85.5564	83.1984	83.6505	39.3770
EP	84.9537	87.7561	85.3982	85.8502	40.4769
GZ	86.1523	88.9547	86.5967	87.0488	41.0762
NHE	86.8436	89.6459	87.2880	87.7401	41.4218
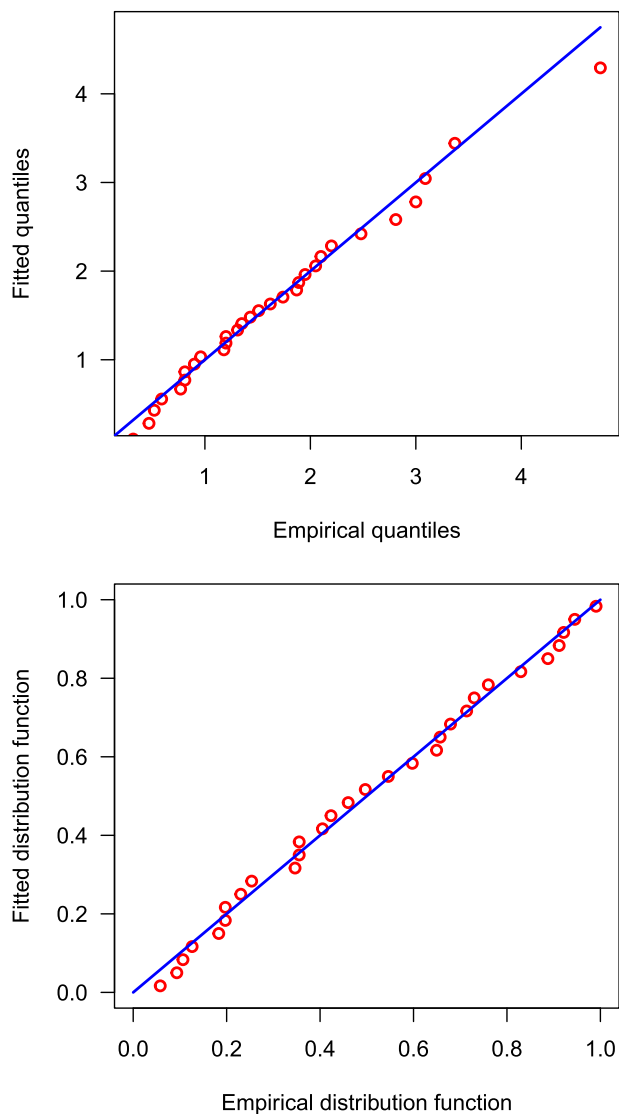
FIGURE 3. Q-Q and P-P plots of ATE distribution.

FIGURE 4. Fitted PDF (left) and estimated CDF (right panel).

TABLE 7. Statistics for goodness-of-fit and associated p-values.

Distribution	W(p-value)	KS(p-value)	A^2(p-value)
ATE	0.1803(0.9950)	0.0600(0.9999)	0.0182(0.9987)
MOEE	0.2125(0.9866)	0.0641(0.9997)	0.0219(0.9955)
EP	0.5166(0.7285)	0.1164(0.8107)	0.0738(0.7320)
GZ	0.6440(0.6060)	0.1149(0.8230)	0.0836(0.6749)
NHE	2.8190(0.0341)	0.2381(0.0666)	0.4905(0.0414)

indicators to evaluate the proposed model's suitability. Figure 3 depicts the ATE distribution's Q-Q plot (theoretical versus empirical quantile) and P-P plot. In Figure 4, we presented the fitted density function of candidate models and an empirical along with the estimated distribution function of ATE distribution. Table 7 displays the W, KS, and A^2 statistics and their associated p-values, which were used to assess the goodness-of-fit of the ATE model in comparison to alternative distributions. Based on the results, the ATE distribution showed the lowest value of test statistics and a higher p-value, indicating that it is a superior fit and produces more reliable and consistent outcomes than the distributions under study.
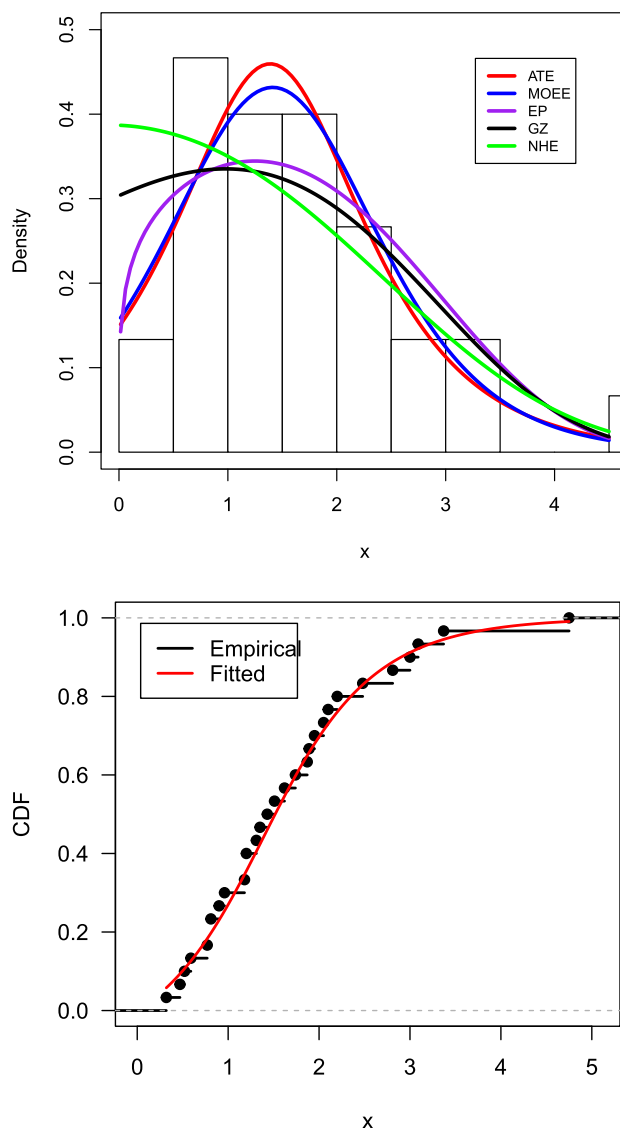
D. DATASET-II

The data set consisting of 34 observations of vinyl chloride in mg/L was taken from surveillance wells for clean-up gradient ground-water [3].

"5.1, 1.2, 1.3, 0.6, 0.5, 2.4, 0.5, 1.1, 8.0, 0.8, 0.4, 0.6, 0.9, 0.4, 2.0, 0.5, 5.3, 3.2, 2.7, 2.9, 2.5, 2.3, 1.0, 0.2, 0.1, 0.1, 1.8, 0.9, 2.0, 4.0, 6.8, 1.2, 0.4, 0.2".

TABLE 8. MLEs with SE.

Distribution	parameter	SE	parameter	SE
$\text{ATE}(\hat{\alpha}, \hat{\lambda})$	0.0018	1.2944	0.5321	0.0913
$\text{MOEEATE}(\hat{\alpha}, \hat{\lambda})$	0.8230	0.4845	0.4819	0.1733
$\text{EPATE}(\hat{\alpha}, \hat{\lambda})$	0.7110	0.0994	0.2790	0.0419
$\text{NHE}(\hat{\alpha}, \hat{\sigma})$	0.9003	0.3442	0.6320	0.4160
$\text{GE}(\hat{\lambda}, \hat{\theta})$	1.0764	0.2474	0.5581	0.1242

TABLE 9. Model selection and goodness-of-fit statistics.

Distribution	KS(p-value)	CVM(p-value)	AD(p-value)	-2logL	AIC	BIC
ATE	0.0890(0.9507)	0.0405(0.9331)	0.2719(0.9574)	110.9052	114.9052	117.9579
MOEE	0.0876(0.9565)	0.0318(0.9716)	0.241(0.9749)	110.7915	114.7915	117.8443
EP	0.1228(0.6840)	0.0927(0.6246)	0.5801(0.6657)	113.7415	117.7415	120.7942
NHE	0.0838(0.9707)	0.0328(0.9679)	0.2417(0.9745)	110.8345	114.8345	117.8872
GE	0.0978(0.9012)	0.0521(0.8668)	0.3179(0.9236)	110.8037	114.8037	117.8565

E. PARAMETER ESTIMATION

For the application of ATE distribution using second data, we have considered four other well-known distributions, and the GZ model is replaced by GE (generalized exponential) distribution due to the problem in estimating its parameters. MLEs along with SE are reported in Table 8 for all competing models

F. MODEL SELECTION

For the second data set, we computed some criteria to choose the best model such as -2logL, AIC, and BIC, and presented in Table 9, and observed that the suggested model ATE performs similar or better than MOEE, EP, NHE, and GE models. Further PP-plot and QQ-plot are also depicted to visualize its performance graphically in Figure 5.

G. GOODNESS-OF-FIT TEST OF ATE DISTRIBUTION

To compare the fit of the ATE distribution to the candidate models MOEE, EP, NHE, and GE, we computed some test statistics and p-values (see Table 9). According to our findings, the ATE model fits the data as well as or better than competing distributions (see Figure 6).

VII. MODEL ANALYSIS UNDER THE BAYESIAN APPROACH

In a Bayesian approach, the analysis of the model involves considering the parameters as random variables rather than constants. Unlike the classical approach, where the likelihood of the data sample is used, Bayesian modeling incorporates prior information to support assumptions about the parameter distribution Gelman et al. [13].

A. PRIOR DISTRIBUTION

In Bayesian analysis, a prior distribution (referred to as the prior) represents our initial beliefs about the true parameter values before considering the data. In this article, we have chosen a Gamma prior to the parameters $\theta = (\alpha, \lambda)$ as $\alpha \sim G(c_1, d_1)$, and $\lambda \sim G(c_2, d_2)$ where $(c_1 = 0.01, d_1 = 0.50)$ and $(c_2 = 0.01, d_2 = 0.75)$, respectively. The Gamma prior described here is widely employed as a weak prior for variance, exhibiting a nearly flat distribution (refer to
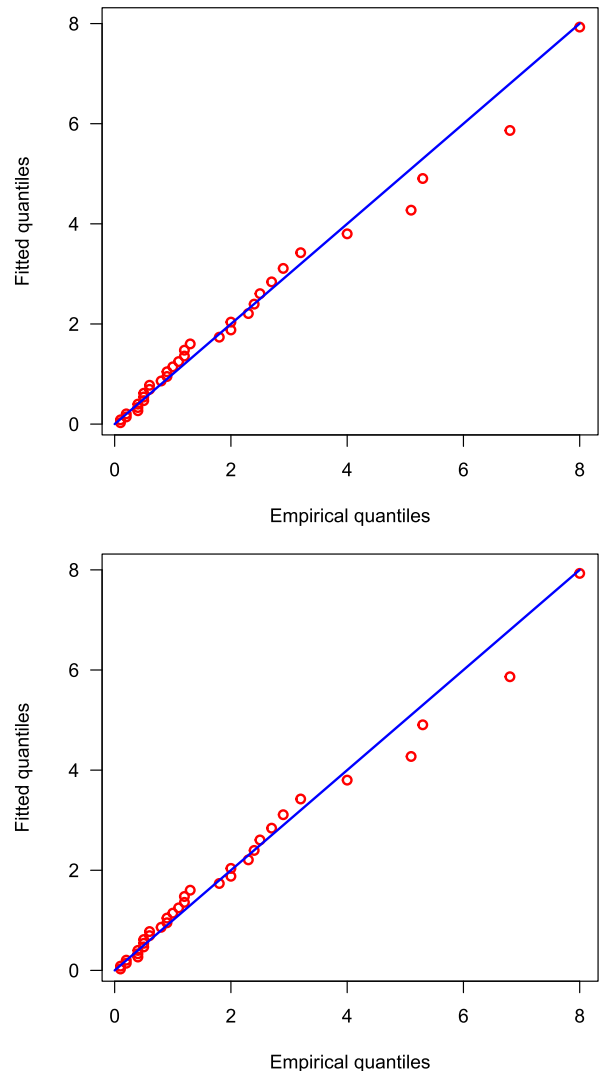

FIGURE 5. Q-Q and P-P plots of ATE distribution.

Figure 7). We can express the prior distributions in the following way

$$p(\alpha) = \frac{d_1^{c_1}}{\Gamma(c_1)} \alpha^{c_1 - 1} \exp(-d_1 \alpha); \ \alpha > 0, \ (c_1, d_1) > 0.$$

$$p(\lambda) = \frac{d_2^{c_2}}{\Gamma(c_2)} \lambda^{c_2 - 1} \exp(-d_2 \lambda); \ \lambda > 0, \ (c_2, d_2) > 0.$$

B. LIKELIHOOD FUNCTION

When we have a dataset $\underline{x} = (x_1, \ldots, x_n)$, we can determine the likelihood function using the following equation,

$$l(\underline{x}|\alpha, \lambda) = n(\log \alpha + \log \lambda) - n \log\{arctan(\alpha)\} - \lambda \sum_{i=1}^{n} x_i$$

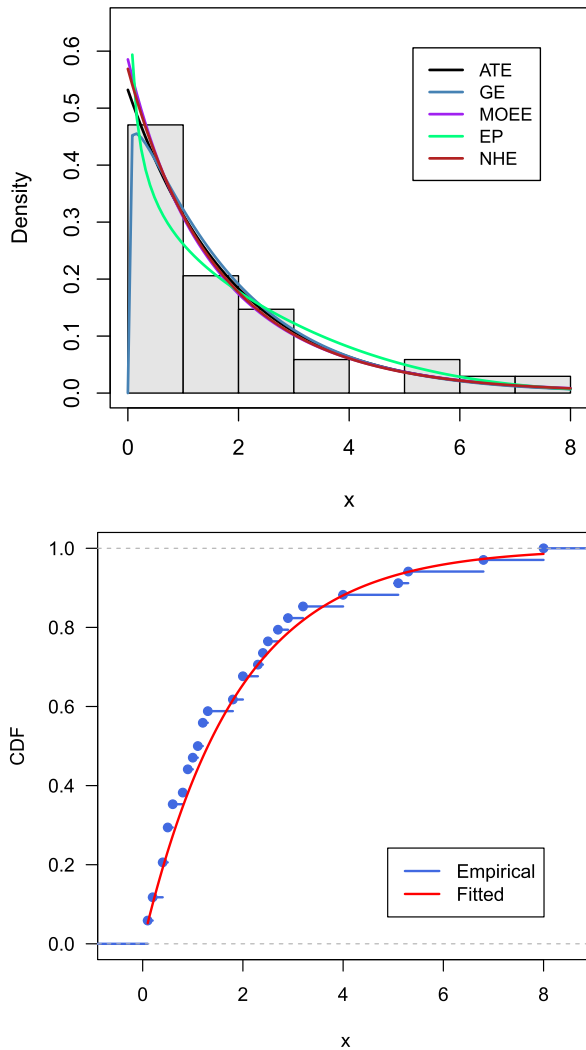$$- \sum_{i=1}^{n} \ln\{1 + [\alpha \exp(-\lambda x_i)]^2\}.$$

FIGURE 6. Fitted PDF (left) and estimated CDF (right panel).

The term $p\left(\alpha, \lambda\right)$ represents the distribution that reflects our prior beliefs about the various parameter values $\theta = \left(\alpha, \lambda\right)$ in our model.

C. POSTERIOR DISTRIBUTION

Under the Bayesian inference approach, Bayes' theorem is utilized to compute the posterior distribution–a probability distribution estimate–which can be represented as follows:
$p\left(\alpha, \lambda/\underline{x}\right) = L\left(\underline{x}|\alpha, \lambda\right) p\left(\alpha\right) p\left(\lambda\right).$

$$p\left(\alpha, \lambda/\underline{x}\right)$$
$$= \left(\frac{\alpha\lambda}{\arctan(\alpha)}\right)^n \prod_{i=1}^{n} \left\{\frac{\exp(-\lambda x_i)}{1 + [\alpha \exp(-\lambda x_i)]^2}\right\}$$
$$\times \frac{d_1^{c_1}}{\Gamma(c_1)} \alpha^{c_1 - 1} \exp\left(-d_1 \alpha\right) \frac{d_2^{c_2}}{\Gamma(c_2)} \lambda^{c_2 - 1} \exp\left(-d_2 \lambda\right).$$
$$p\left(\alpha, \lambda/\underline{x}\right)$$
$$\propto \frac{\alpha^{n+c_1-1} \lambda^{n+c_2-1}}{\arctan^n(\alpha)} \prod_{i=1}^{n} \left\{\frac{\exp(-\lambda x_i - d_1 \alpha - d_2 \lambda)}{1 + [\alpha \exp(-\lambda x_i)]^2}\right\}.$$
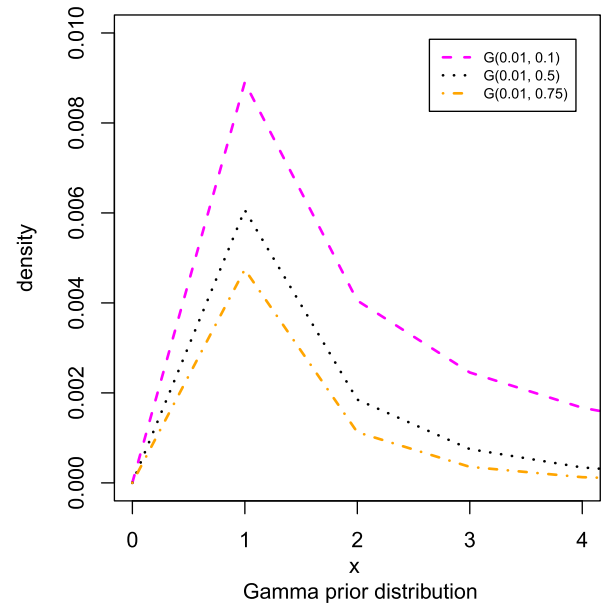

FIGURE 7. Gamma prior to some parameter's values.

The posterior distribution contains all essential information for Bayesian analyses, and the goal is to derive numerical and graphical summaries by means of integration. However, the posterior distribution can be rather complex, making it challenging to draw any meaningful inferences. Therefore, we propose an alternative approach called the simulation technique. This technique relies on the utilization of the Markov Chain Monte Carlo (MCMC) approach. MCMC generates samples by operating a cleverly designed Markov Chain that ultimately reaches convergence towards the desired target distribution, namely the posterior distribution $p\left(\alpha, \lambda/\underline{x}\right)$. There are various techniques available for constructing such chains. Some of these techniques include the Gibbs sampler see [10] and [14] which are specific instances within the general framework introduced by Metropolis et al. [27] and Hasting [18]. In this article, we employ MCMC algorithms implemented through Stan (Stan Development team) [40]. Specifically, we utilize the HMC algorithm and its adaptive variant NUTS. For more details, please refer to the works of [4] and [20]. Recently, Sapkota [35] presented a Bayesian analysis using the HMC/NUTS sampler.

D. SAMPLING METHOD
1) NO-U-TURN SAMPLER (NUTS):
The NUTS engine autonomously calculates the most suitable value for the leapfrog step size, denoted as L, during each iteration. The primary objective is to enhance the distance traversed at every L while simultaneously regulating the stochastic traversal pattern. Let θ_0 and θ_1 denote the initial and current positions of a particle, respectively, while D signifies half the displacement between θ_0 and θ_1 achieved at each leapfrog step. The primary objective entails the iterative execution of leapfrog steps until the position θ_1 commences

TABLE 10. Informational statistic of sampler parameters.

chains	accept_stat	stepsize	treedepth	n_leapfrog	divergent	energy
All chains	0.9316	0.2454	2.4606	8.0532	0	45.5748
chain1	0.9044	0.3678	2.2360	6.2530	0	45.6982
chain2	0.9289	0.2746	2.3970	7.4280	0	45.6536
chain3	0.9546	0.1475	2.7290	10.2950	0	45.4878
chain4	0.9383	0.1917	2.4805	8.2370	0	45.4594

TABLE 11. Summary of posterior samples for the ATE distribution.

parameter	mean	se_mean	sd	n_eff	Rhat	CI	HPD
alpha	2.3559	0.0373	1.3385	1287	1.0015	(0.0217, 5.1931)	(0.0000204, 4.680)
lambda	0.9092	0.0059	0.2074	1226	1.0018	(0.5187, 1.3023)	(0.5080, 1.2900)
log-posterior	-44.5854	0.0519	1.5163	852	1.0031	(-48.855, -43.1922)	(-47.8756, -43.1603)

retrogressing towards θ_0. This aim is effectively realized through the application of a well-defined algorithm, wherein leapfrog steps are undertaken until the temporal derivative of the half-displacement D exhibits negativity.

$$\frac{\partial D}{\partial t} = \frac{\partial}{\partial t} \left[\frac{1}{2} (\theta_1 - \theta_0)^T (\theta_1 - \theta_0) \right] = (\theta_1 - \theta_0)^T p < 0.$$

However, this algorithm does not guarantee convergence or reversibility to the target distribution. To address this issue, NUTS employs a doubling method for slice sampling, as introduced by Neal [32]. For more detailed information about NUTS, refer to Hoffman and Gelman [20], as well as Nishio and Arkawa [33].

2) HAMILTONIAN MONTE CARLO (HMC) METHOD

Hamiltonian Monte Carlo (HMC) exhibits a higher computational cost compared to Metropolis and Gibbs sampling methods. However, HMC's proposals demonstrate significantly enhanced efficiency Gelman, Lee, and Guo [13]. Consequently, HMC necessitates fewer samples for exploring the posterior distribution.

3) CONVERGENCE AND EFFICIENCY DIAGNOSTICS FOR NUTS/ HMC SAMPLING

We utilized the initial dataset provided in the application section to analyze the model ATE under Bayesian. To conduct the analysis, we employed Stan software that employs NUTS sampler, which is a variant of HMC simulation, see Hoffman and Gelman [20]. Our implementation involved running Stan with the HMC algorithm and the NUTS engine, utilizing four chains, and iterating over 4000 iterations. During the convergence assessment, we make observations regarding the performance of both NUTS/HMC and MCMC techniques

i) NUTS/ HMC: In this study, we examine the details regarding divergence, `step_size`, `tree_depth`, `energy`, and `acceptance statistic`. For more information, please refer to the publication by Betancourt [2] and the user manual of Stan (Stan Development team) [40].

ii) MCMC: The MCMC draws may be observed by creating visual representations of the following graphs. such as autocorrelation plots, trace plots, pairs plots, etc. Figure 8 displayed here are autocorrelation plots for alpha and lambda, representing all chains. Autocorrelation measures the relationship between samples in a Monte Carlo simulation
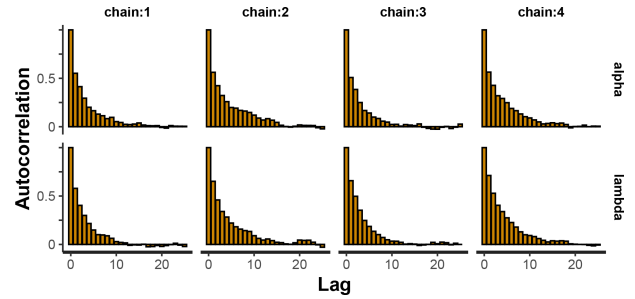

FIGURE 8. Autocorrelation histograms for α and λ across all chains.
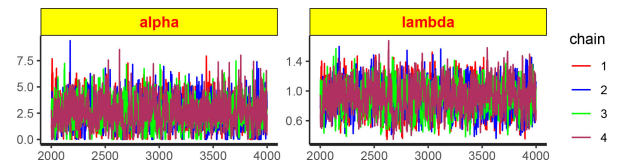

FIGURE 9. Trace plot for α and λ for all chains.
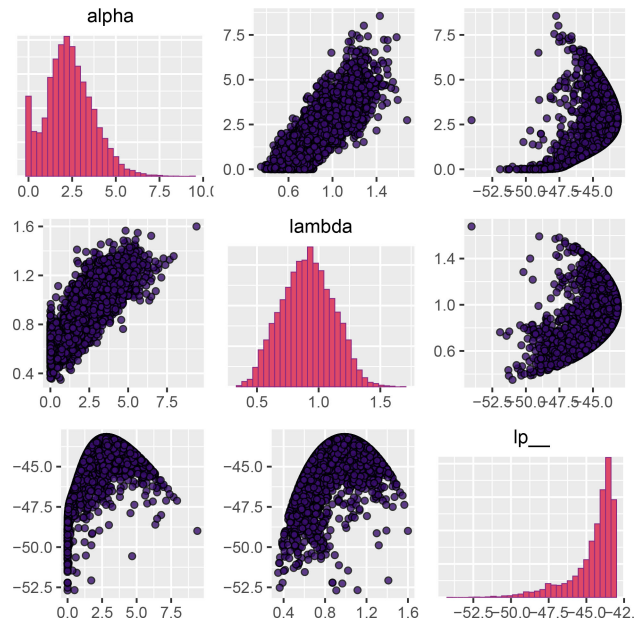

FIGURE 10. Pairs plot for α, λ and log-posterior.

for more information see Vehtari et al. [42]. The illustration in Figure 9 presents trace plots that effectively demonstrate the favorable characteristics of mixing, stationarity, and convergence for alpha and lambda variables across all chains. Trace plots serve as invaluable tools for visually scrutinizing the behavior of the sampling process and assessing the uniformity of convergence within multiple chains. Figure 10 presents a pairs plot displaying the alpha, lambda, and log-posterior MCMC samples. The diagonal of the plot consists of univariate marginal posteriors represented by histograms. Above and below the diagonal, bivariate plots are displayed as scatter plots. Table 10 depicts the statistics relating to the efficiency of the MCMC sampling.
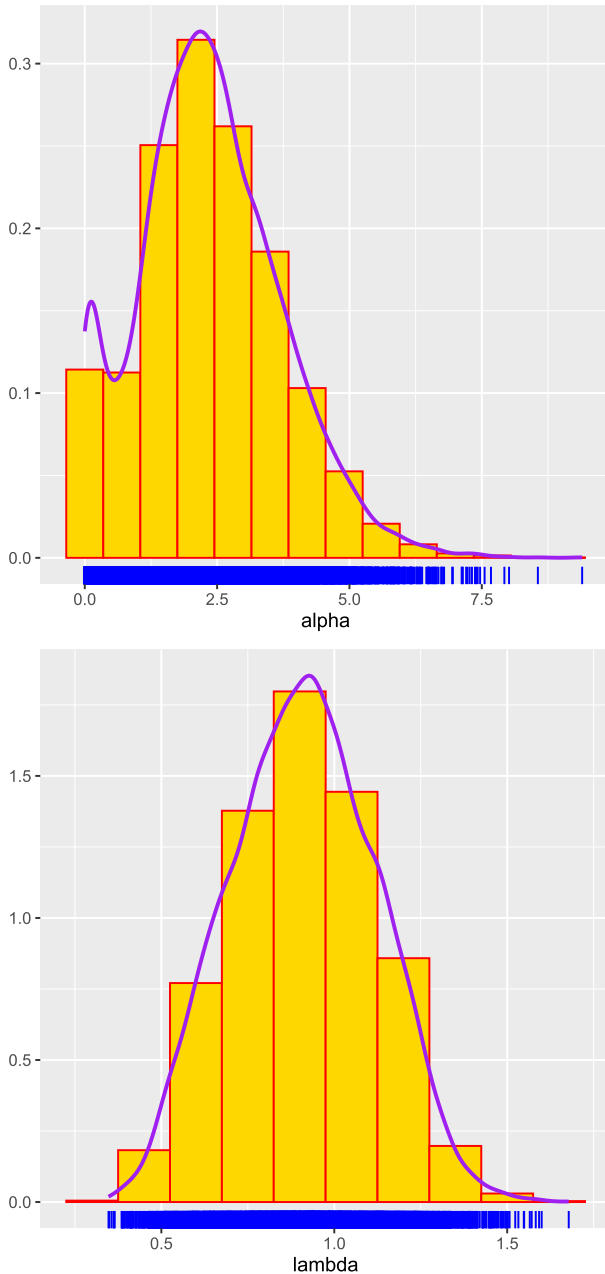
FIGURE 11. Histogram with kernel density estimates for α and λ.

FIGURE 12. Histograms of y and replicated datasets $y_{rep}[1]$, $y_{rep}[15]$ and $y_{rep}[30]$.

E. POSTERIOR ANALYSIS

1) NUMERICAL SUMMARY

Utilizing the R-Software in combination with the `rstan` package (as documented in [39]), we have effectively derived the posterior density for the fitted ATE model. The posterior summary for all merged chains is provided in Table 11, encompassing evaluations of the posterior mean, standard error of the mean ($se_{m}ean$), posterior standard deviation (sd), a 95% credible interval (CI), and the highest posterior density (HPD). Additionally, it is worth noting that the efficiency of the samples is indicated by the fact that the number of effective samples ($n_{e}ff$) utilized for posterior mean estimation surpasses 10% of the total sample size. The efficacy of the
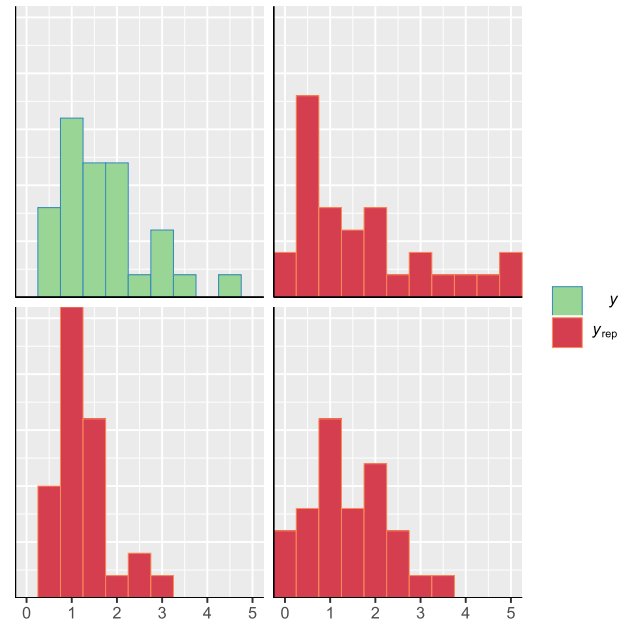
sampling process is further supported by the `Rhat` statistic (estimated potential scale reduction), which registers a value below 1.1.

2) VISUAL SUMMARY

We have created a histogram with a kernel density estimate for alpha and lambda (Figure 11) using all 4 chains. These graphical representations offer comprehensive information about the posterior samples and their corresponding parameters. In total, 8000 posterior samples were utilized to generate these graphs. Notably, the parameter lambda demonstrates near symmetry, while alpha displays positive skewness.

F. POSTERIOR PREDICTIVE CHECKS (PPCS)

A common approach to evaluating the adequacy of a Bayesian model is by assessing the agreement between the model's predictions and the observed data [11], [12]. If our model effectively captures the data, it should generate simulated data that closely resemble the observed data. The PPCs utilize simulated data from the posterior predictive distribution (PPD) to assess model fit. The R Bayes plot package provides a range of plotting functions designed to facilitate the visualization of posterior predictive checks. These visual representations can be generated using both observed and generated posterior predictive distribution (PPD) data. For further details, readers are directed to the work by Gabry et al. as outlined in [9]. The distribution of the outcome variable implied by a model, known as the PPD, is obtained by updating our beliefs about unknown parameters $\theta = (\alpha, \lambda)$ based on the observed data y (N=30). The PPC for y_{rep}
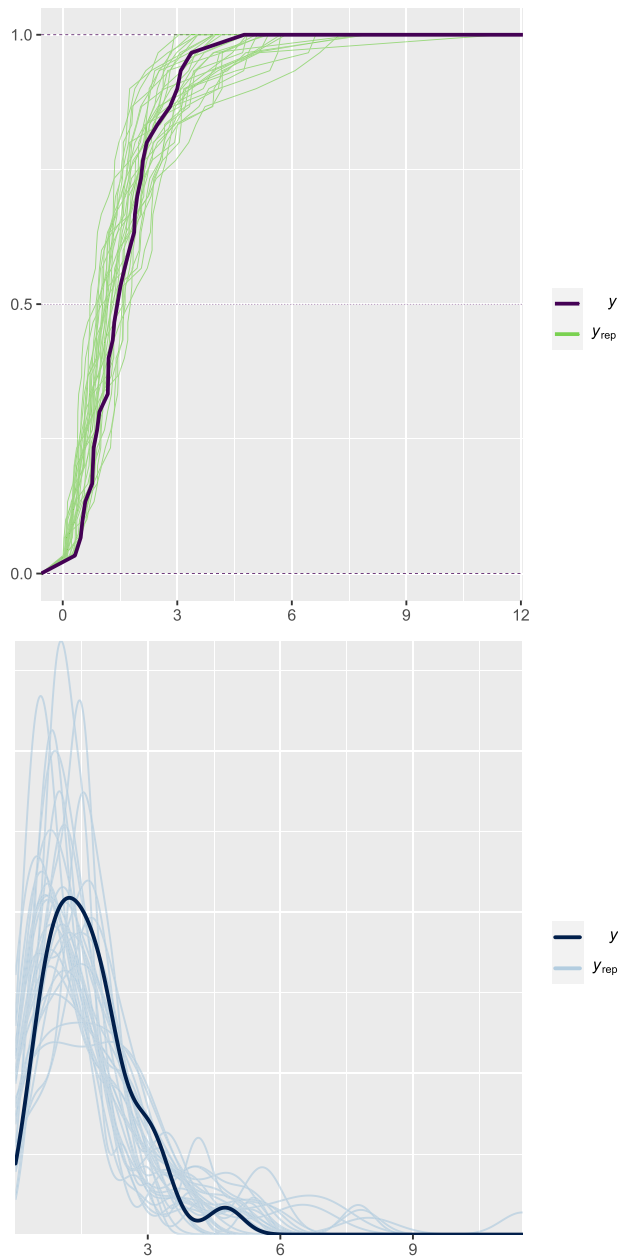
FIGURE 13. Fitted CDF with simulated CDF (left) and density of y and simulated data (right).

observation can be generated using

$$p\left(\tilde{y}/y\right) = \int p\left(\tilde{y}/\theta\right)p\left(\theta/y\right)d\theta.$$

For every iteration within the simulation index s, spanning from 1 to S, the posterior distribution $\theta(s) \sim p(\theta|y)$ of the model parameters is subjected to analysis. Within this context, a vector of N outcomes, denoted as $\tilde{y}^s$, is generated through the simulation process, wherein data is synthesized from the data model, conditioned on the identified parameters. This sequential procedure forms a matrix encompassing S rows and N columns, thereby yielding an $S \times N$
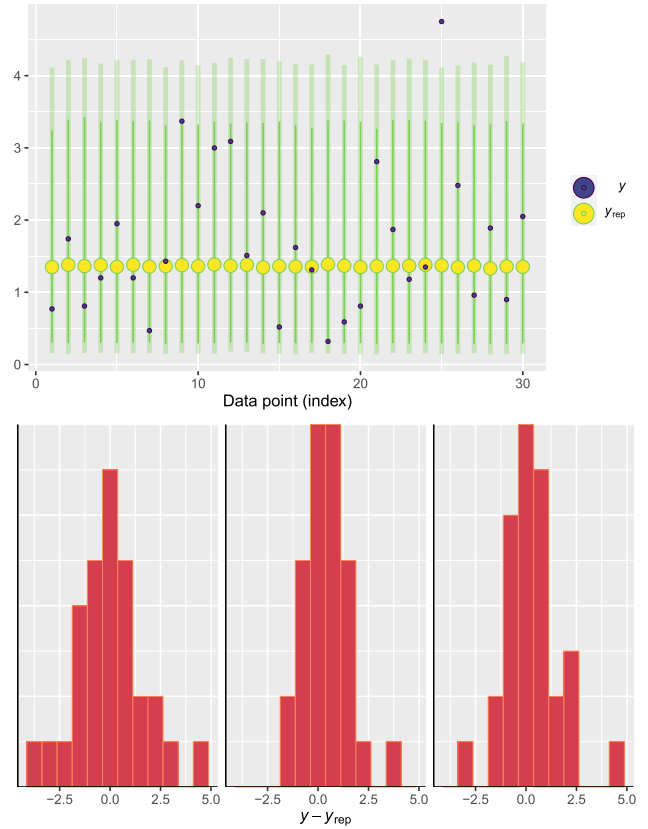

FIGURE 14. Interval plot (left) and histogram of posterior predictive error (right).

(or 8000×30) matrix of drawn values. It is important to emphasize that this matrix, derived from the simulation process, represents duplications or replications of the existing observed data y instead of predictive estimations tailored for forthcoming observations. To enhance our comprehension of the decision concerning the study of PPC, we examine the three replicated observations: the smallest ($y_{rep}[1]$), the middle ($y_{rep}[15]$), and the largest ($y_{rep}[30]$). We have provided visual summaries to assess the predictive capabilities of posterior samples. These summaries include a histogram (Figure 12), the estimates of empirical CDF for each dataset y_{rep} are superimposed with the distribution of y (represented in dark) in Figure 13, left panel while in right panel kernel density estimates. To provide a clearer understanding, we have incorporated an interval plot see Figure 14 in the left panel. This plot effectively illustrates intervals using vertical bars, emphasizing the inner 80% and outer 90% HPD intervals. Moreover, the plot utilizes data points to indicate the medians, with darker points representing observed values of y. Figure 14 showcases a histogram, featured in the right panel, that illuminates the predictive errors derived from both the observed data y and the synthesized data instances $y_{rep}[1]$, $y_{rep}[15]$, and $y_{rep}[30]$. This visual representation provides a comprehensive insight into the disparities between the actual observed data and the outcomes generated from the model.

VIII. CONCLUSION

In conclusion, this research paper introduced the arctan exponential distribution as a continuous distribution with two parameters. The statistical and mathematical properties of the suggested distribution were extensively explored, including the hazard rate, cumulative hazard rate, moments, incomplete moments, reliability function, quantile function, entropies, order statistics, Lorenz and Bonferroni curves, and symmetry measures such as skewness and kurtosis. The maximum likelihood estimation (MLE) method was employed to estimate the distribution parameters, and a numerical simulation experiment was conducted to assess the stability and consistency of the MLEs. Real-world data sets were used to demonstrate the significance of the proposed distribution, and various test statistics were computed to evaluate its applicability and potential. The results showed that the arctan exponential distribution performed comparably or better than other lifetime models considered.

Furthermore, a Bayesian analysis of the arctan exponential distribution was conducted using the Stan software, employing the No-U-Turn sampler (NUTS) based on Markov chain Monte Carlo (MCMC) techniques. This adaptive variant of Hamiltonian Monte Carlo (HMC) offered a robust and efficient sampling method. The chains were found to be well mixed and converged through numerical and graphical analysis. The model parameters were estimated, and posterior predictive checks confirmed the model's ability to generate reliable samples. These Bayesian techniques were successfully applied to an observed dataset, enabling a comprehensive Bayesian analysis of the arctan exponential distribution in the context of the research. This research aimed to provide an alternative model for probability theory, survival analysis, and applied statistics.

ACKNOWLEDGMENT

REFERENCES

[1] Z. Y. Al-Jammal, "Exponentiated exponential distribution as a failure time distribution," *IRAQI J. Stat. Sci.*, vol. 8, no. 14, pp. 63–75, Dec. 2008.

[2] M. Betancourt, "A conceptual introduction to Hamiltonian Monte Carlo," 2017, *arXiv:1701.02434*.

[3] D. K. Bhaumik, K. Kapur, and R. D. Gibbons, "Testing parameters of a gamma distribution for small samples," *Technometrics*, vol. 51, no. 3, pp. 326–334, Aug. 2009.

[4] B. Carpenter, A. Gelman, M. D. Hoffman, D. Lee, B. Goodrich, M. Betancourt, M. Brubaker, J. Guo, P. Li, and A. Riddell, "Stan: A probabilistic programming language," *J. Stat. Softw.*, vol. 76, no. 1, pp. 1–32, 2017.

[5] A. K. Chaudhary, L. P. Sapkota, and V. Kumar, "Truncated Cauchy power–exponential distribution: Theory and applications," *IOSR J. Math.*, vol. 16, no. 6, pp. 44–52, 2020.

[6] A. K. Chaudhary, L. P. Sapkota, and V. Kumar, "Some properties and applications of Arctan generalized exponential distribution," *Int. J. Innov. Res. Sci., Eng., Technol.*, vol. 10, no. 1, pp. 456–468, 2021.

[7] G. M. Cordeiro, E. M. Ortega, and A. J. Lemonte, "The exponential–Weibull lifetime distribution," *J. Stat. Comput. Simul.*, vol. 84, no. 12, pp. 2592–2606, 2014.

[8] J. Felip, N. Ahuja, and O. Tickoo, "Tree pyramidal adaptive importance sampling," 2019, *arXiv:1912.08434*.

[9] J. Gabry, D. Simpson, A. Vehtari, M. Betancourt, and A. Gelman, "Visualization in Bayesian workflow," 2017, *arXiv:1709.01449*.

[10] A. E. Gelfand and A. F. M. Smith, "Sampling-based approaches to calculating marginal densities," *J. Amer. Stat. Assoc.*, vol. 85, no. 410, pp. 398–409, Jun. 1990.

[11] A. Gelman, "A Bayesian formulation of exploratory data analysis and goodness-of-fit testing," *Int. Stat. Rev.*, vol. 71, no. 2, pp. 369–382, Aug. 2003.

[12] A. Gelman, J. B. Carlin, H. S. Stern, and D. B. Rubin, *Bayesian Data Analysis*. London, U.K.: Chapman & Hall, 1995.

[13] A. Gelman, D. Lee, and J. Guo, "Stan: A probabilistic programming language for Bayesian inference and optimization," *J. Educ. Behav. Statist.*, vol. 40, no. 5, pp. 530–543, Oct. 2015.

[14] S. Geman and D. Geman, "Stochastic relaxation, Gibbs distributions, and the Bayesian restoration of images," *IEEE Trans. Pattern Anal. Mach. Intell.*, vol. PAMI-6, no. 6, pp. 721–741, Nov. 1984.

[15] E. Gómez-Déniz and E. Calderín-Ojeda, "Modelling insurance data with the Pareto ArcTan distribution," *ASTIN Bulletin, J. IAA*, vol. 45, no. 3, pp. 639–660, 2015.

[16] R. D. Gupta and D. Kundu, "Theory & methods: Generalized exponential distributions," *Austral. New Zealand J. Statist.*, vol. 41, no. 2, pp. 173–188, 1999.

[17] R. D. Gupta and D. Kundu, "A new class of weighted exponential distributions," *Statistics*, vol. 43, no. 6, pp. 621–634, Dec. 2009.

[18] W. K. Hastings, "Monte Carlo sampling methods using Markov chains and their applications," *Biometrika*, vol. 57, no. 1, pp. 97–109, Apr. 1970.

[19] D. Hinkley, "On quick choice of power transformation," *J. Roy. Stat. Soc. C, Appl. Statist.*, vol. 26, no. 1, pp. 67–69, 1977.

[20] M. D. Hoffman and A. Gelman, "The No-U-Turn sampler: Adaptively setting path lengths in Hamiltonian Monte Carlo," *J. Mach. Learn. Res.*, vol. 15, no. 1, pp. 1593–1623, Apr. 2014.

[21] E. G. M. Hui, *Learn R for Applied Statistics*. New York, NY, USA: Springer, 2019.

[22] A. Mo. Isa, S. O. Bashiru, B. A. Ali, A. A. Adepoju, and I. I. Itopa, "Sine-exponential distribution: Its mathematical properties and application to real dataset," *UMYU Scientifica*, vol. 1, no. 1, pp. 127–131, Sep. 2022.

[23] F. Jamal and C. Chesneau, "The sine Kumaraswamy-G family of distributions," *J. Math. Extension*, vol. 15, no. 2, pp. 1–33, 2020.

[24] R. Joshi, L. Sapkota, and V. Kumar, "The logistic-exponential power distribution with statistical properties and applications," *Int. J. Emerg. Technol. Innov. Res.*, vol. 7, no. 12, pp. 629–641, 2020.

[25] F. Llorente, L. Martino, D. Delgado-Gómez, and G. Camps-Valls, "Deep importance sampling based on regression for model inversion and emulation," *Digit. Signal Process.*, vol. 116, Sep. 2021, Art. no. 103104.

[26] A. Marshall, "A new method for adding a parameter to a family of distributions with application to the exponential and Weibull families," *Biometrika*, vol. 84, no. 3, pp. 641–652, Sep. 1997.

[27] N. Metropolis, A. W. Rosenbluth, M. N. Rosenbluth, A. H. Teller, and E. Teller, "Equation of state calculations by fast computing machines," *J. Chem. Phys.*, vol. 21, no. 6, pp. 1087–1092, 1953.

[28] J. J. A. Moors, "A quantile alternative for kurtosis," *J. Roy. Stat. Soc. D, Statistician*, vol. 37, no. 1, pp. 25–32, 1988.

[29] D. Murthy, M. Xie, and R. Jiang, *Weibull Models*. New York, NY, USA: Wiley, 2003.

[30] S. Nadarajah and F. Haghighi, "An extension of the exponential distribution," *Statistics*, vol. 45, no. 6, pp. 543–558, Dec. 2011.

[31] R. M. Neal, "Annealed importance sampling," *Statist. Comput.*, vol. 11, pp. 125–139, Apr. 2001.

[32] R. M. Neal, "Slice sampling," *Ann. Statist.*, vol. 31, no. 3, pp. 705–767, Jun. 2003.

[33] M. Nishio and A. Arakawa, "Performance of Hamiltonian Monte Carlo and No-U-Turn sampler for estimating genetic parameters and breeding values," *Genet. Selection Evol.*, vol. 51, no. 1, pp. 1–12, Dec. 2019.

[34] *R: A Language and Environment for Statistical Computing*, R Found. Stat. Comput., R Core Team, Vienna, Austria, 2023.

[35] L. P. Sapkota, "A Bayesian analysis and estimation of Weibull inverse Rayleigh distribution using HMC method," *Nepal J. Math. Sci.*, vol. 3, no. 2, pp. 39–58, Nov. 2022.

[36] M. Shrahili, I. Elbatal, W. Almutiry, and M. Elgarhy, "Estimation of sine inverse exponential model under censored schemes," *J. Math.*, vol. 2021, Oct. 2021, Art. no. 7330385.

[37] R. M. Smith and L. J. Bain, "An exponential power life-testing distribution," *Commun. Statist.*, vol. 4, no. 5, pp. 469–481, Jan. 1975.

[38] L. Souza, W. Junior, C. De Brito, C. Chesneau, T. Ferreira, and L. Soares, "On the Sin-G class of distributions: Theory, model and application," *J. Math. Model.*, vol. 7, no. 3, pp. 357–379, 2019.

[39] *RStan: The R Interface to Stan*, Stan Development Team, R Package document Version 2.21.5, 2022.

[40] *The Stan Core Library*, document Version 2.30.0, Stan Development Team, 2023.

[41] L. Tomy, G. Veena, and C. Chesneau, "The sine modified Lindley distribution," *Math. Comput. Appl.*, vol. 26, no. 4, p. 81, Dec. 2021.

[42] A. Vehtari, A. Gelman, D. Simpson, B. Carpenter, and P.-C. Bürkner, "Rank-normalization, folding, and localization: An improved R̂ for assessing convergence of MCMC (with discussion)," *Bayesian Anal.*, vol. 16, no. 2, pp. 667–718, Jun. 2021.

LAXMI PRASAD SAPKOTA received the M.Sc. degree in statistics from Tribhuvan University, Kathmandu, Nepal. He is currently a dedicated Research Scholar specializing in statistics with DDU Gorakhpur University, Gorakhpur, India. He is also an Assistant Professor in statistics with Tribhuvan University, Tribhuvan Multiple Campus, Palpa, Nepal, where he has been imparting his extensive knowledge for over 14 years. His wealth of teaching experience has made him a respected figure in the domain of statistics education. Driven by a passion for exploring statistical phenomena, his primary research interests include the array of compelling topics, such as in-depth investigations into probability distributions and applied statistics, and a keen focus on cutting-edge areas, such as Bayesian statistics and actuarial science. His innovative contributions to these areas have the potential to reshape the landscape of statistical applications.

ARWA M. ALSAHANGITI received the Graduate degree from the Department of Statistics, Necmettin Erbakan University, in 2021. She is currently pursuing the master's degree with the Faculty of Science, Department of Statistics, Selçuk University, Konya, Turkey. Her research interests include distribution theory and regression models.

VIJAY KUMAR received the Ph.D. degree in statistics from DDU Gorakhpur University, Gorakhpur, India. He is currently a Distinguished Professor and the esteemed Head of the Department of Mathematics and Statistics, DDU Gorakhpur University. With an impressive teaching and research journey spanning 29 years, he has become a notable figure in the academic realm. His expertise extends globally, as he also serves as a Visiting Faculty with the esteemed MaxPlanck-Institute, Germany. His research interests include diverse range of fields, prominently focusing on probability distribution, reliability engineering, Bayesian statistics, and actuarial science. His commitment to advancing these disciplines has not only led to groundbreaking contributions but has also earned him recognition as a guiding force in the academic community. His dedication to nurturing young talents is evident through his mentorship. He has successfully guided and supervised the research endeavors of 11 accomplished Ph.D. scholars, each contributing to the academic landscape. Currently, he continues to impart his knowledge and expertise to three promising Ph.D. scholars under his guidance.

AHMED M. GEMEAY received the M.Sc. degree in statistics from Tanta University, Tanta, Egypt, in 2020. He is currently an Assistant Lecturer in statistics and mathematics with the Department of Mathematics, Faculty of Science, Tanta University. His current research interests include the generalized classes of distributions and their special models.

M. E. BAKR received the Ph.D. degree in mathematical statistics from the Mathematics Department, Faculty of Science, Al-Azhar University, Cairo, Egypt, in 2018. His research interests include the theory of reliability, the classes of life distributions, censored data, and statistical inference.

OLUWAFEMI SAMSON BALOGUN is currently a Postdoctoral Researcher with the School of Computing, University of Eastern Finland, Kuopio, Finland. His research interests include data mining, machine learning, learning analytics, biostatistics, and probability distribution models.

ABDISALAM HASSAN MUSE was born in Borama, Somalia, in 1988. He received the bachelor's degree in mathematics and physics from the Faculty of Science, Amoud University, Borama, in 2012, the M.Sc. degree in mathematics and statistics from the School of Postgraduate Studies and Research, Amoud University, in 2017, and the Ph.D. degree in statistics from the Institute of Basic Science, Technology and Innovation, Pan African University, hosted at the Jomo Kenyatta University of Agriculture and Technology, Nairobi, Kenya, in 2022. He is currently the Head of the Faculty of Science and Humanities, School of Postgraduate Studies and Research, Amoud University. His research interests include applied statistics, survival analysis, Bayesian statistics, distribution theory, disease mapping, spatial statistics, and regression modeling. He is a maintainer of three R packages, and he has over 30 refereed journal articles published or accepted and serves as a reviewer for several journals. He received the Post Graduate African Union Scholarship Award during his Ph.D. (statistics) Program.

● ● ●